

Accepted Manuscript

A tumor-targeted Ganetespib-zinc phthalocyanine conjugate for synergistic chemo-photodynamic therapy

Liangfeng Huang, Gaofei Wei, Xiaoqi Sun, Yali Jiang, Zeqian Huang, Yanjuan Huang, Yifeng Shen, Xiaoyu Xu, Yunhui Liao, Chunshun Zhao



PII: S0223-5234(18)30320-9

DOI: [10.1016/j.ejmech.2018.03.077](https://doi.org/10.1016/j.ejmech.2018.03.077)

Reference: EJMECH 10342

To appear in: *European Journal of Medicinal Chemistry*

Received Date: 2 February 2018

Revised Date: 8 March 2018

Accepted Date: 26 March 2018

Please cite this article as: L. Huang, G. Wei, X. Sun, Y. Jiang, Z. Huang, Y. Huang, Y. Shen, X. Xu, Y. Liao, C. Zhao, A tumor-targeted Ganetespib-zinc phthalocyanine conjugate for synergistic chemo-photodynamic therapy, *European Journal of Medicinal Chemistry* (2018), doi: 10.1016/j.ejmech.2018.03.077.

This is a PDF file of an unedited manuscript that has been accepted for publication. As a service to our customers we are providing this early version of the manuscript. The manuscript will undergo copyediting, typesetting, and review of the resulting proof before it is published in its final form. Please note that during the production process errors may be discovered which could affect the content, and all legal disclaimers that apply to the journal pertain.

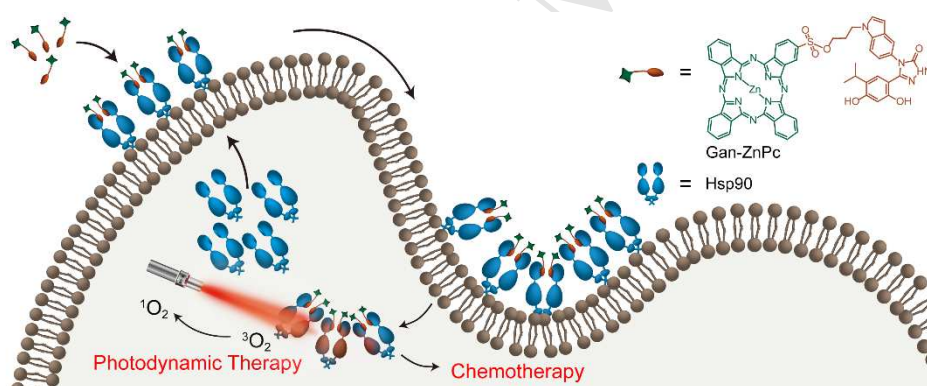
A Tumor-targeted Ganetespib-Zinc Phthalocyanine Conjugate for Synergistic Chemo-Photodynamic Therapy

Liangfeng Huang,[‡] Gaofei Wei,^{‡*} Xiaoqi Sun, Yali Jiang, Zeqian Huang, Yanjuan Huang, Yifeng Shen, Xiaoyu Xu, Yunhui Liao and Chunshun Zhao*

School of Pharmaceutical Sciences, Sun Yat-sen University, Guangzhou, 510006, People's Republic of China

*Corresponding Author: E-mail: zhaocs@mail.sysu.edu.cn, Tel: +86 20 39943118

Graphical abstract



**A Tumor-targeted Ganetespib-Zinc Phthalocyanine
Conjugate for Synergistic Chemo-Photodynamic Therapy**

Liangfeng Huang,[‡] Gaofei Wei,^{‡} Xiaoqi Sun, Yali Jiang, Zeqian Huang, Yanjuan
Huang, Yifeng Shen, Xiaoyu Xu, Yunhui Liao and Chunshun Zhao**

School of Pharmaceutical Sciences, Sun Yat-sen University, Guangzhou, 510006,

People's Republic of China

*Corresponding Author: E-mail: zhaocs@mail.sysu.edu.cn, Tel: +86 20 39943118

[‡]These authors contributed equally to this work.

Abstract

Therapeutic effects of photodynamic therapy (PDT) are limited by the selectivity of photosensitizer (PS). Herein, a novel tumor-targeted drug-PS conjugate (Gan-ZnPc) which integrated with zinc phthalocyanine (ZnPc) and Ganetespib has been developed. ZnPc is a promising PS with remarkable photosensitization ability. Ganetespib is a heat shock protein 90 (Hsp90) inhibitor with preferential tumor selectivity and conjugated to ZnPc as a tumor-targeted ligand. The multifunctional small molecule conjugate, Gan-ZnPc, could be bound to extracellular Hsp90 and then selectively internalized into the tumor cells, followed by the generation of abundant intracellular reactive oxygen species (ROS) upon irradiation. Besides, Gan-ZnPc can arrest cell proliferation and induce apoptosis by the inhibition of Hsp90. Herein, with combination of the inhibition of Hsp90 and the generation of cytotoxic ROS, Gan-ZnPc implements tumor selectivity, concentrated PDT and chemotherapy in a synergistic manner, which results in highly effective anti-tumor activity *in vitro* and *in vivo*.

Key words: Zinc phthalocyanine; Heat shock protein 90; Tumor-targeted; Photodynamic therapy; Chemotherapy

1. Introduction

Photodynamic therapy, which has been approved for clinical use, is a promising noninvasive treatment for cancer. It combines three intrinsically nontoxic components (photosensitizer, light and tissue oxygen) to generate cytotoxic reactive oxygen species which leads to oxidative damage of the cells construction and triggered an apoptotic or necrotic response[1-3]. PDT reactions can be controlled externally because these biological responses only occur in where the PS located and is restricted by the light irradiation to the diseased tissue[4, 5]. Although PDT has been extensively studied during recent years and preclinical practices have shown promising results, it is still less commonly used for cancer therapy in clinic. The main reason is that PS without tumor selectivity is difficult to accumulate in malignant tissue[6], which causes undesirable adverse effects, such as skin photosensitivity and photoallergic reactions during PDT[7, 8]. Thus, it is critical to selectively localize PS in tumor to enhance PDT efficiency and minimize collateral damage to normal tissue. Therefore, development of PS with improved targeting specificity to avoid off-target sensitization has been proven challenging.

Previously, for achieving enhanced PS selectivity, nanomedicine was commonly applied strategy to increase the specific accumulation at the target site. The major underlying mechanism of nanomedicines is the enhanced permeability and retention (EPR) effect, whereby defects or gaps in the tumor vasculature allow the extravasation and accumulation of larger particles that would be retained within the

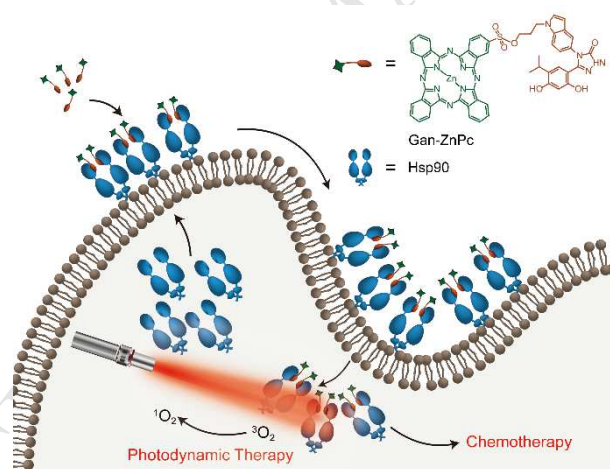
blood vessels of healthy tissues[9]. Unfortunately, further penetration of these same large particles is often hampered by the dense extracellular matrix, leading to problems with the delivery of nanoparticles to cells deep within a tumor mass[10, 11]. However, the recent clinical development of multiple low-molecular weight ligand–drug conjugates suggests that these small molecule conjugates could be a promising strategy to delivery drugs to target site. Besides, these ligand-drug small molecule conjugates are often advantaged in their antigenicity, in vivo and in vitro stability, ability to penetrate tumors and ease and cost of manufacturing[12, 13]. Moreover, a ligand-drug conjugate only with tumor selectivity may be not efficient enough for anti-tumor therapy. Recently, there has been considerable interest in combining different anticancer therapeutic methods. The combination acting on different disease pathways has shown several advantages and considerably enhanced therapeutic efficacy[14, 15].

In the present work, a novel tumor-targeted drug-PS conjugate was developed (scheme 1). This conjugate could selectively bind to Hsp90, a target receptor overexpressed in tumor cells, leading to enhanced accumulation of PS in tumor cells for enhanced PDT and chemotherapy. As a proof-of-concept study, zinc phthalocyanine (ZnPc) was utilized as a characteristic PS, which has a strong absorption in the tissue-penetrating red-light wavelength range and high efficiency in generating ROS, but in lack of tumor selectivity[16, 17]. As a tumor-targeted drug, Ganetespib (termed STA-9090), an attractive Hsp90 inhibitor, was chosen because of

its high affinity for activated Hsp90 in tumor cells and low affinity for latent Hsp90 in normal cells[18-20]. Hsp90 is known to be a molecular chaperone with intracellular and extracellular overexpression in malignant tumor cells and highly restricted expression within normal tissue[21, 22]. Therefore, cell-surface expression of Hsp90 and the high affinity with its inhibitors in tumor cells allow Hsp90-targeted drugs to concentrate in tumor tissue without harming healthy tissue[13]. Also, Hsp90 participates in many key processes in oncogenesis such as self-sufficiency in growth signals, stabilization of mutant proteins, angiogenesis, and metastasis[23, 24]. As a Hsp90 inhibitor, Ganetespib can potently arrest cell proliferation and induce apoptosis in a wide variety of human tumor cell lines[25]. With the conjugation of Ganetespib and ZnPc, Gan-ZnPc could concentrate in tumor cells due to binding to activated extracellular Hsp90 secreted by tumor cells and promote the cellular internalization of Gan-ZnPc by an active endocytotic process[26-28]. The concentration of PS inside the cells was of great benefit to the generation of intracellular ROS with the irradiation, thereby an enhanced PDT effect could be expected[29]. Furthermore, A. Ferrario et al. had previously reported that PDT alone was found to induce expression of various pro-survival and angiogenic signaling molecules such as HIF-1 α , survivin and VEGF, etc. in tumor tissue and weaken its efficacy. However, inhibition of activated Hsp90 in tumor cells resulting in the blockade of multiple signal transduction cascades was a beneficial adjuvant for PDT in a synergistic way[30, 31].

The combination of two or more therapeutic modalities was helpful in overcoming limitations encountered by each therapy when used alone[32].

According to the results in this study, Gan-ZnPc was demonstrated preferential internalization into MCF7 tumor cells mediated by Hsp90 via receptor blocking experiments. The dark- and photo-toxicity against MCF7 cells and mice bearing 4T1 xenograft revealed that Gan-ZnPc exhibited potent in vitro and in vivo anti-tumor effect due to the combination of tumor-targeted chemotherapy and concentrated PDT in tumor tissue. To the best of our knowledge, this study is the first example of a PS conjugated with a Hsp90 inhibitor to enhance tumor selectivity and implement PDT and chemotherapy for synergistic anti-tumor therapy.



Scheme 1. Chemical structure and schematic illustration of Gan-ZnPc for synergistic tumor-targeted chemotherapy and PDT. Gan-ZnPc was firstly bound to extracellular Hsp90 and then selectively internalized into the tumor cells. The accumulation of Gan-ZnPc could inhibit the action of Hsp90 and generate intracellular ROS upon irradiation. With the combination of these therapeutic

modalities, Gan-ZnPc was a multifunctional molecular containing a promising synergistic chemo-photodynamic therapy.

2. Results and discussions

2.1 Synthesis of Gan-ZnPc

Gan-ZnPc was synthesized through conjugating sulfonic ZnPc and Ganetespib with an aliphatic chain. Ganetespib was synthesized according to previous reports[33] and ZnPc was sulfonated for its later modification. A propane aliphatic linkage was attached to Ganetespib with exposure of an amino group. After sulfamide reaction, Gan-ZnPc was successfully synthesized and used for further experiments. W. Ying et al. have confirmed that Ganetespib bound to Hsp90 through important hydrogen bonding interactions involving the resorcinol hydroxyl group, carbonyl group of triazolone and the N² of triazolone[25]. In our study, ZnPc was conjugated to aminoindole of Ganetespib to maintain the affinity to Hsp90. But, the phthalocyanine derivatives in our study were not able to be characterized by ¹H NMR and HPLC presumably due to their aggregation[34]. Therefore, we used MALDI-TOF and FTIR spectrum to characterize it. As showed in Figure S1, the FTIR spectrum of Gan-ZnPc demonstrated that the stretching vibrations of -C=C-, -C=N-, -C-N- and -CH in benzene are around 1629, 1329, 1087 and 2958 cm⁻¹ respectively, which were the representative peaks of ZnPc segment. Moreover, the stretching vibrations of -OH, -NH- and -C=O are around 3389, 3219 and 1704 cm⁻¹ respectively, which were the representative peaks of Ganetespib segment. Comparing the FTIR spectrum of

compound S6 and Gan-ZnPc, the appearance of stretching vibrations of -OH around 3389 cm^{-1} suggested the hydrolysis of the benzyl. Herein, the FTIR spectrum of Gan-ZnPc suggested that Ganetespib was successfully conjugated to ZnPc.

2.2 Spectroscopy property of Gan-ZnPc

Most PS have a great absorbance at Q-band which enabled them to be excited by long-wavelength light with high penetrability. Herein, the UV/vis absorbance of ZnPc, Ganetespib and Gan-ZnPc were detected and compared (Figure 1A). ZnPc demonstrated the expected characteristic absorption peaks at 672 nm in DMSO. On the contrary, Ganetespib has none absorbance at Q-band. When ZnPc was covalently conjugated to Ganetespib, the slight red shift of the absorbance to 678 nm at Q-band was noticed. This change may be caused by the modification of ZnPc with electron withdrawing group. The differences between ZnPc and Gan-ZnPc in fluorescence spectroscopy were similar with the UV/vis spectroscopy. As shown in Figure 1B, the maximum excitation wavelength of ZnPc was at 672 nm while Gan-ZnPc was at 678 nm, which was corresponded to the maximum absorption wavelength. As for emission fluorescence (Figure 1C), the maximum emission wavelength of ZnPc and Gan-ZnPc was at 678 nm and 688 nm respectively. These results indicated that Gan-ZnPc had a similar spectroscopy property to ZnPc and suggested that Gan-ZnPc may have a parallel photosensitivity of ZnPc.

2.3 ROS generation efficiency

ROS generation was measured by using DPBF as a ROS indicator. DPBF could capture and react with ROS and reduce its absorbance at 416 nm. Through recording the degradation rate of DPBF, the generation efficiency of ROS was measured (Figure 1D). Obviously, there was no significant degradation of DPBF without the PS, which suggested that ROS can't be generated without PS upon irradiation. However, DPBF was degraded rapidly when ZnPc or Gan-ZnPc was existed, which demonstrated that ZnPc and Gan-ZnPc generated plenty of ROS after laser irradiation at 671 nm. More than 90% of DBPF was degraded after 80 s accumulatively irradiation and the degradation rate was rapidly decreased probably due to the reducing concentration of DBPF. Obviously, there is no significant influence on ROS generation after the modification of ZnPc, revealing the promising ROS generation efficiency of Gan-ZnPc.

2.4 Photosensitization ability in aqueous solutions

Although Gan-ZnPc can dissolve in aqueous solutions containing 1% DMSO in a certain concentration, aggregation of PS was still a problem resulting in losing their photosensitization ability such as fluorescence property and generation of ROS. However, it has been reported that the aggregation of PS can be disassociated by proteins under physiological environment[35]. To quantitatively measure the monomer percentage in aqueous solutions, the fluorescence emission comparison method was used since the monomers emit fluorescence while the emission of dimers or multimers can be neglected. As ZnPc can dissolve and disperse absolutely in

DMSO, the monomer percentage was defined to 100% and the fluorescence emission intensity of ZnPc dissolved in aqueous solution was normalized. As shown in Figure 1E, Gan-ZnPc dissolved in PBS containing 1% DMSO emitted inappreciable fluorescence compared to dissolve in pure DMSO. This phenomenon indicated that most Gan-ZnPc dissolved in aqueous solutions was in a state of self-aggregation and lost photosensitization ability. When fetal bovine serum (FBS) was added to the solution, the emission intensity was increased. The monomer percentage was increased to 19% and 36% when 5% and 10% FBS contained in PBS respectively. The recuperative fluorescence with addition of FBS indicated that Gan-ZnPc may interact with FBS and disperse in monomer state which resulted in recovering their photosensitization ability. By the way, an inconspicuous blueshift of fluorescence peak of Gan-ZnPc could be observed due to the interaction between the Gan-ZnPc and proteins, which is similar to previously reports[35]. The further confirmation of ROS generation of Gan-ZnPc in aqueous solution was measured. As shown in Figure 1F, Gan-ZnPc dissolved in aqueous solution containing higher concentration of FBS possessed higher ROS generation efficiency with the laser irradiation, which was consistent with the fluorescence emission intensity. Furthermore, comparison of ROS generation efficiency between Gan-ZnPc and ZnPc in aqueous solution showed insignificant difference (Figure S4), indicating they have an equivalent ROS generation efficiency in aqueous solution. The considerable percentage of monomers of Gan-ZnPc and considerable ROS generation efficiency in serum protein contained

systems implied Gan-ZnPc could be used for PDT under protein-rich physiological environment.

2.5 Photostability

Furthermore, a PS used in PDT needs to be stable enough after irradiation, so that it can generate enough cytotoxic ROS during the treatment. For confirming the photostability of Gan-ZnPc and ZnPc, their characteristic maximal absorption in Q-band was used to quantify their concentration and their photobleaching property was demonstrated. As shown in Figure S5, after 20 min irradiation at a laser irradiation intensity of 100 mW cm^{-2} at 671 nm, only about 10% of Gan-ZnPc and ZnPc was photobleached, which indicating that Gan-ZnPc was stable enough to be used in PDT.

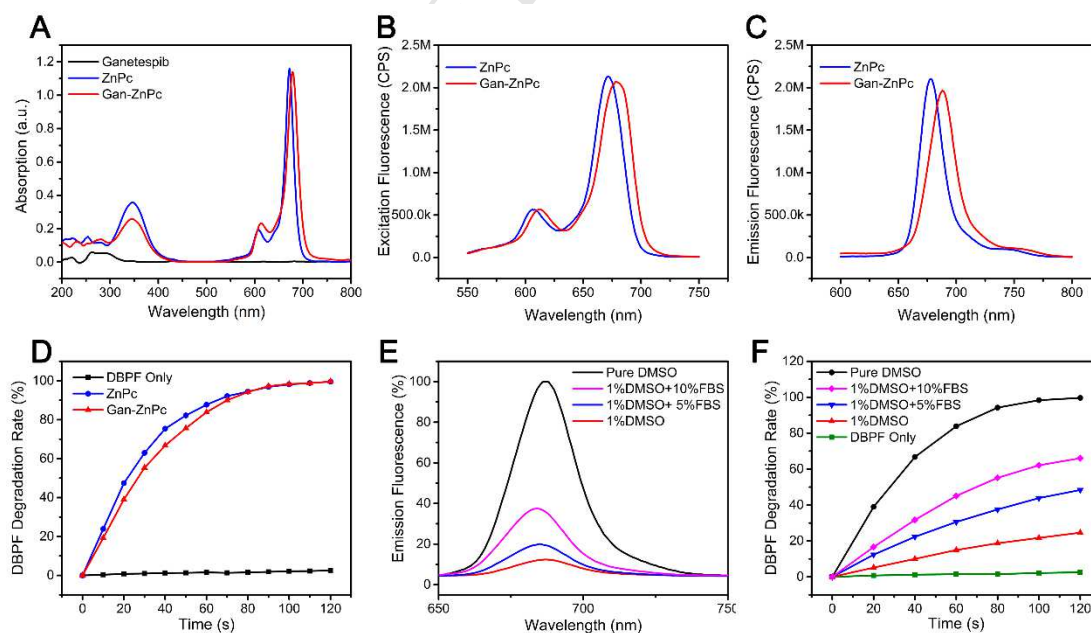


Figure 1. Spectroscopy and photosensitization ability of Gan-ZnPc. (A) UV/Vis absorption spectra of Ganetespib, ZnPc and Gan-ZnPc in DMSO (5 μM). Excitation

(B) and Emission (C) fluorescence spectroscopy of ZnPc and Gan-ZnPc in DMSO (3 μM). (D) ROS generation of ZnPc and Gan-ZnPc in DMSO (1 μM) under laser irradiation indicated by the degradation rate of DBPF (normalized absorbance at 416 nm). Emission fluorescence spectroscopy (E) and ROS generation (F) of Gan-ZnPc in pure DMSO and aqueous solution containing 1% DMSO and different concentration of FBS.

2.6 Cellular internalization and cellular ROS generation

Cellular internalization profiles were evaluated on MCF7 and NIH/3T3 cell using confocal laser scanning microscopy (CLSM). MCF7 is human breast cancer cell with high Hsp90 expression while NIH/3T3 is murine embryonic fibroblast cells used as normal cell model. As expected, MCF7 cells incubated with Gan-ZnPc for 2 h and 4 h showed stronger fluorescence compared to ZnPc, indicating that more Gan-ZnPc was internalized into MCF7 cells (Figure 2A & Figure S6A). Comparing the fluorescence intensity of 2 h and 4 h incubation, both ZnPc and Gan-ZnPc displayed a time-dependent cellular internalization. To confirm cellular internalization was mediated by Hsp90, 100 folds molar of free Ganetespib, which can block the binding between Hsp90 and Gan-ZnPc, was mixed in culture medium with Gan-ZnPc. It was obviously that the fluorescence was decreased after incubation for 2 h or 4 h compared with Gan-ZnPc, suggesting that cellular uptake of Gan-ZnPc was decreased significantly when Hsp90 was occupied by free Ganetespib. To further confirm the increased cellular internalization of Gan-ZnPc was achieved by binding to Hsp90

expressed on the cell surface, NIH/3T3 was used as a negative control. As shown in Figure 2B & Figure S6B, it was obviously that weak fluorescence was observed in both ZnPc and Gan-ZnPc after 2 h or 4 h incubation, and there is no significant difference between them, indicating a small amount of ZnPc or Gan-ZnPc was internalized. The difference in cellular internalization of ZnPc and Gan-ZnPc between the MCF7 and NIH/3T3 cells demonstrated the preferential tumor cellular internalization of Gan-ZnPc, which may be attributed to the expression of Hsp90 on the surface of tumor cells. To quantify the cellular internalization, flow cytometry (FCM) analysis was carried out on MCF7 cells and NIH/3T3 cells and showed in Figure 2 C&D. Gan-ZnPc showed significantly more cellular internalization compared to ZnPc or the mixture of Ganetespib and Gan-ZnPc, which was consistent with the results of CLSM. The high cellular internalization of Gan-ZnPc mediated by Hsp90 indicated that Gan-ZnPc could concentrate in tumor cells with high Hsp90 expression, which was potential to improve PDT effect.

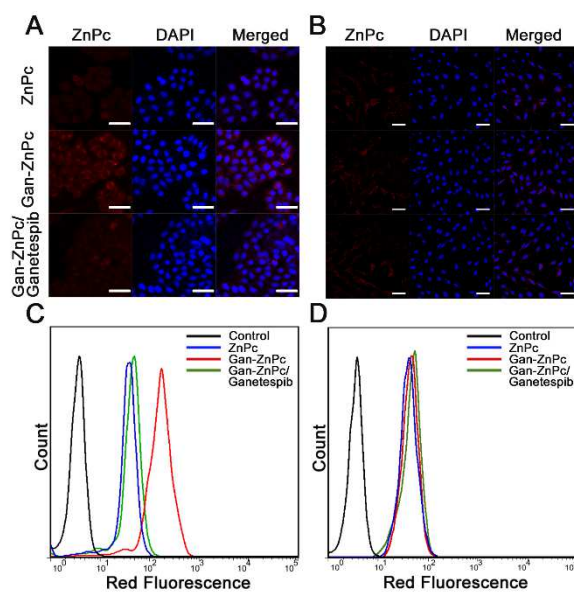


Figure 2. Cellular internalization evaluation by CLSM and FCM. CLSM images of MCF7 cells (A) and NIH/3T3 cells (B) after incubation with ZnPc, Gan-ZnPc or Gan-ZnPc/GanetespiB mixture for 4 h and stained with DAPI. Flow cytometry analysis of MCF7 cells (C) and NIH/3T3 cells (D) after different incubation for 4 h. (scale bar = 50 μm)

Additionally, the intracellular ROS generation ability of Gan-ZnPc in living cells was detected using DCFH-DA as an indicator. The higher DCF fluorescence was corresponded to the higher intracellular ROS generation. As shown in Figure 3A, compared to ZnPc or the mixture of GanetespiB and Gan-ZnPc, Gan-ZnPc exhibited a greater intracellular ROS generation in MCF7 cells, while showed negligible difference in NIH/3T3 cells (Figure 3B). The results of intracellular ROS generation determined by DCF fluorescence was consistent with the cellular internalization

studies, indicating that the more cellular internalization, the more intracellular ROS generation, which may result in the higher cytotoxicity.

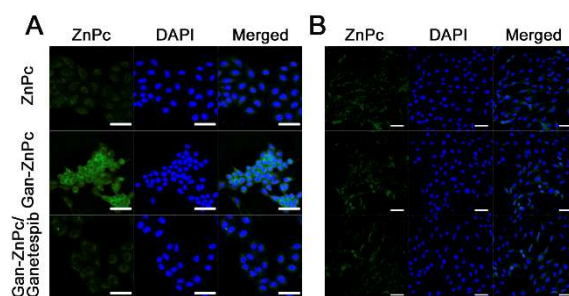


Figure 3. Intracellular DCF fluorescence imaged of MCF7 cells (A) and NIH/3T3 cells (B) after incubation with ZnPc, Gan-ZnPc or Gan-ZnPc/Ganetespi mixture for 4 h and irradiation. (scale bar = 50 μ m)

2.7 In vitro Cytotoxicity Study

The in vitro cytotoxicity of Gan-ZnPc against MCF7, 4T1, NIH/3T3 was evaluated by MTT assay. Firstly, cytotoxicity of Gan-ZnPc against MCF7 was evaluated for totally 24 h, 48 h and 72 h incubation. For totally 24 h incubation, cells were incubated with drug solution for 6 h first and exposed to irradiation for 10 min at 6 h, 9 h and 12 h, and then incubated till reached 24 h. Similarly, for 48 h group, cells were incubated with drug solution for 12 h first and exposed to irradiation at 12 h, 18 h and 24 h. For 72 h group, cells were incubated with drug solution for 24 h first and exposed to irradiation at 24 h, 30 h and 36 h. As illustrated in Figure 4, cell viability decreased along with the increasing concentration, which demonstrated the cytotoxicity of Ganetespi, ZnPc and Gan-ZnPc were dose-dependent. Upon irradiation, Ganetespi/ZnPc equimolar mixture was relatively more potent than Ganetespi or ZnPc alone, which may benefit from the combination of PDT and inhibition of

Hsp90. However, cell viability was inhibited to less than 20% by 100 nM of Gan-ZnPc with irradiation in 24 h (Figure 4A) indicating that Gan-ZnPc possessed the higher cytotoxicity against MCF7 cells than Ganetespib/ZnPc equimolar mixture. This may be due to the more internalization of Gan-ZnPc into MCF7 cells than ZnPc which resulted in enhancing PDT efficacy. In addition, the *in vitro* cytotoxicity evaluation was carried out without irradiation (Figure 4D), the free ZnPc didn't show significant cytotoxicity during the assay. As for Ganetespib, there is no significant difference in the absence and presence of irradiation, which proving that irradiation played a negligible role in cell viability without the PS. However, in the absence of irradiation, Gan-ZnPc also exhibited certain dark toxicity which may be attributed to the inhibition of Hsp90 in MCF7 cells. But it was noticeable that the dark toxicity of Gan-ZnPc is slightly lower than Ganetespib, which was likely due to the bulky PS of Gan-ZnPc and the reduced affinity to Hsp90. Furthermore, the cytotoxicity of Gan-ZnPc was evaluated in 48 h (Figure 4 B&E) and 72 h (Figure 4 C&F). To further characterize that Gan-ZnPc was an "all in one" molecule, *in vitro* cellular cytotoxicity was also evaluated on 4T1 cells. As showed in Figure S7, Gan-ZnPc was more potential than Ganetespib/ZnPc equimolar mixture and these results was similar to the evaluation on MCF7 cells. Therefore, the *in vitro* cytotoxicity on MCF7 and 4T1 cells suggested that Gan-ZnPc was a potential molecule used for synergistic chemo-photodynamic therapy.

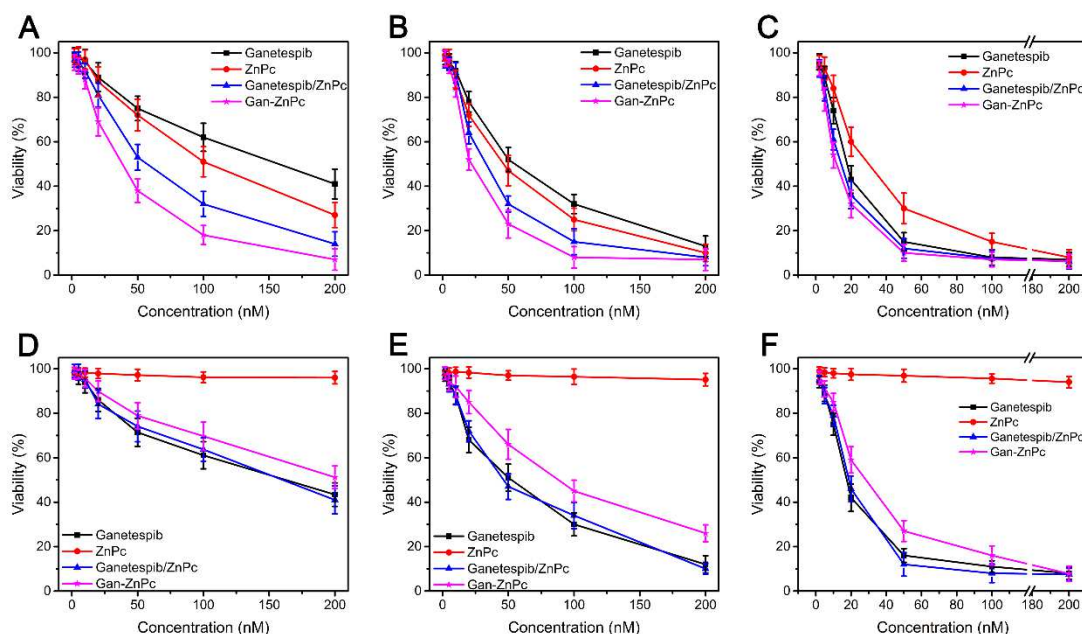


Figure 4. Comparison of the in vitro cytotoxicity of ZnPc, Ganetespiib, Ganetespiib/ZnPc (equimolar mixture) and Gan-ZnPc on MCF7 cells for 24 h (A), 48 h (B) and 72 h (C) in the presence of irradiation and for 24 h (D), 48 h (E) and 72 h (F) in the absence of irradiation. (red-light LED lamp, 100 mW cm^{-2} , 660-670 nm). Data are expressed as mean \pm standard deviation (SD). (n=6)

To confirm the cell cytotoxicity of Gan-ZnPc differed from tumor cells and normal cells, in vitro cytotoxicity assay was also carried out on the 4T1 and NIH/3T3 cells for 24 h (Figure 5). In the present of irradiation, the aggressive 4T1 cells were more impressionable compared to the non-oncogenic NIH/3T3 cells due to the high affinity to activated Hsp90 and high internalization through binding to the extracellular Hsp90. However, Gan-ZnPc possessed certain phototoxicity to NIH/3T3 cells upon irradiation which may be attributed to the free diffusion into the cells. The negligible toxicity to NIH/3T3 cells in the absent of irradiation suggested that Hsp90

in normal cells was in a latent and uncomplex state with low affinity to the Gan-ZnPc. The *in vitro* cytotoxicity results suggested that covalent conjugation of Ganetespib to ZnPc interestingly promoted the cellular internalization of PS to enhance PDT effect and made Gan-ZnPc a multifunctional molecule with high cytotoxicity against tumor cells while sparing normal cells.

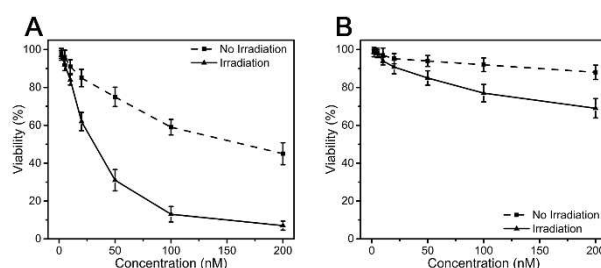


Figure 5. Cytotoxicity evaluation of Gan-ZnPc on 4T1 (A) and NIH/3T3 (B) cells for 24 h with and without irradiation. (red-light LED lamp, 100 mW cm^{-2} , 660-670 nm). Data are expressed as mean \pm standard deviation (SD). (n=6)

2.8 *In vivo* and *ex vivo* biodistribution

Next, *in vivo* biodistribution of Gan-ZnPc and ZnPc was evaluated by fluorescence imaging on unhairing area using 4T1 bearing mice. As shown in Figure 6A, after single intravenous administration, ZnPc was distributed without significant tumor selectivity and the fluorescence of ZnPc was decreased during 24 h. On the contrast, Gan-ZnPc obviously accumulated in the tumor tissue after intravenous injection. Besides, although the fluorescence of Gan-ZnPc of normal tissue near tumor was decreased rapidly during 24 h, the fluorescence in the tumor region was decreased slowly and even maintained a strong fluorescence in 24 h compared to ZnPc. The accumulation of Gan-ZnPc in tumor tissue was similar to Ganetespib, which

possessed a half-life of 58.3 h in tumor[18], indicating that Gan-ZnPc was preferentially distributed to tumor and maintained a high concentration in tumor.

To investigate the distribution of Gan-ZnPc and ZnPc in major organs, mice were sacrificed at 24 h post-injection and the major organs were excised for imaging (Figure 6B). Ex vivo fluorescence images showed a higher fluorescence intensity at the tumor site than other organs in mice which were treated with Gan-ZnPc. Although Gan-ZnPc was distributed in liver and lung, the controllable irradiation to tumor tissue may restrict the adverse effect to the major organs. Additionally, mean fluorescence intensity (MFI) of excised major organs and tumor was shown in Figure 6C. The MFI of Gan-ZnPc in excised tumor was dramatically 2.3 times higher than ZnPc at 24 h post injection. These results confirmed that Gan-ZnPc could successfully accumulate and remain in tumor, which may effectively enhance the PDT efficacy with irradiation in vivo.

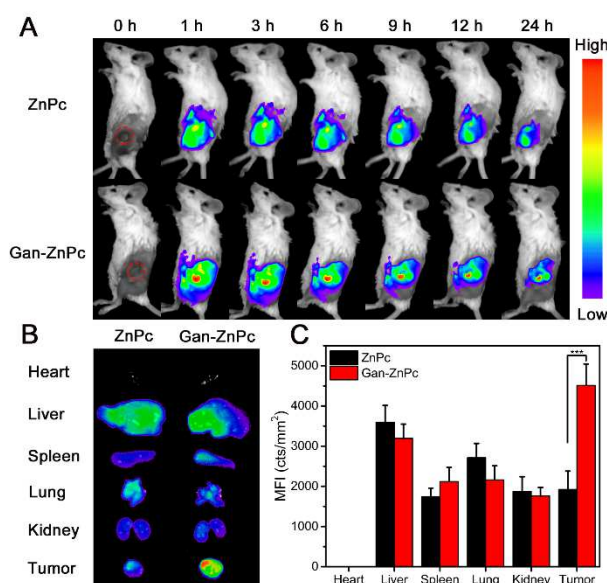


Figure 6. In vivo and ex vivo biodistribution studies on balb/c mice bearing 4T1 xenografts. (A) In vivo fluorescence images on unhairing area of 4T1 bearing mice at different time after single intravenous injection of ZnPc or Gan-ZnPc. (B) Ex vivo fluorescence images of excised major organs and tumor at 24 h post-injection (C) MFI of excised major organs and tumor at 24 h post-injection. Data are expressed as mean \pm standard deviation (SD). (n=3, ***p < 0.001)

2.9 In vivo antitumor efficacy

The in vivo antitumor efficacy of Gan-ZnPc was investigated on balb/c mice bearing 4T1 xenografts. When the tumor grew to about 100 mm³, they were separated randomly into eight groups and intravenously injected with Saline, Ganetespib, ZnPc and Gan-ZnPc respectively. The volume of tumor was measured every two days. As illustrated in Figure 7A, the tumors were completely suppressed for the treatment of Gan-ZnPc with laser irradiation. Such a superiority should be benefited from the selective accumulation of Gan-ZnPc in tumor due to the Hsp90 mediated cellular

internalization, following by the combination of efficient PDT and the inhibition of Hsp90, the more PS accumulated in tumor, the more efficient PDT was. Furthermore, even in the absence of laser irradiation, Gan-ZnPc exhibited a certain anticancer activity, which was ascribed to the inhibition of Hsp90 action in the tumor cells. On the contrary, ZnPc possessed negligible anticancer effect without laser irradiation compared to with laser irradiation. Upon completion of the PDT treatment, all the mice were sacrificed and all the tumors were excised and gathered for imaging (Figure 7B) and weighing (Figure 7C). During the PDT treatment, body weight was also monitored and no significant weight changes were observed compared to the control groups, suggesting that Gan-ZnPc did not induce significant adverse effects on the mice (Figure 7D).

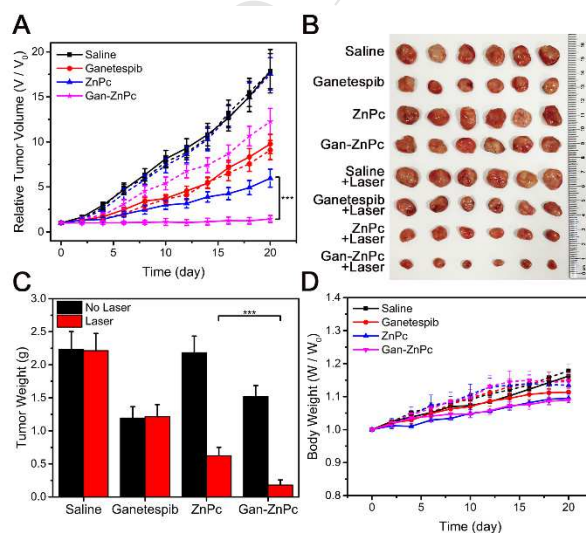


Figure 7. In vivo anti-tumor evaluation on balb/c mice bearing 4T1 xenografts. (A) The relative tumor volume (V/V_0) during the treatment of Saline, ZnPc, Ganetespiib and Gan-ZnPc with or without laser irradiation (500 mW cm^{-2} , 671 nm). Photograph (B) and weight (C) of the tumors excised from the mice bearing 4T1 tumor after PDT

treatment. (D) The relative body weight of mice during the PDT treatment. Data are expressed as mean \pm standard deviation (SD). (solid line for irradiation, dash line for no irradiation, n=6, ***p < 0.001)

3. Conclusions

In summary, Gan-ZnPc, as an “all in one” molecule, could combine Hsp90 inhibition with PDT. Gan-ZnPc could identify and bind to Hsp90 secreted on the tumor cells surface, then entered the cells by Hsp90 mediated cellular internalization. Since Gan-ZnPc concentrating in tumor cells, abundant cytotoxic ROS could generate intracellularly and damage susceptible organelles while triggered by the light. Besides, Gan-ZnPc could inhibit Hsp90 activity in the tumor cells, leading to cell apoptosis. Consequently, under irradiation, Gan-ZnPc was a promising PS with preferable cellular internalization, enhanced tumor accumulation and combination of PDT and chemotherapy. All these superior characteristics of Gan-ZnPc resulted in facilitating anti-tumor efficiency and showed that Gan-ZnPc was a highly promising tumor-targeted drug-PS conjugate for synergistic tumor-targeted chemotherapy and PDT to breast cancers. Our study inspired that conjugating Hsp90 inhibitor with a PS for synergistically implementing tumor-targeted PDT and chemotherapy is an effective means for cancer therapy. Furthermore, the detailed mechanisms of synergistic action of PDT and Hsp90 inhibition of this conjugate are under investigation.

4. Materials and methods

4.1 Materials

Zinc phthalocyanine (ZnPc), chlorosulfonic acid, 2',7'-Dichlorofluorescein diacetate (DCFH-DA), 3-(4,5-dimethyl-thiazol-2-yl)-2,5-diphenyl tetrazolium bromide (MTT), Fetal Bovine Serum (FBS), Dulbecco's modified Eagle's medium (DMEM), phosphate buffered saline (PBS), 1-Boc-5-Aminoindole, 4-isopropylresorcinol, Ganetespib (STA-9090) were purchased from Sigma-Aldrich (USA). Phenyl chloroformate, 3-Bromo-1-propanol, 4',6-Diamidino-2-phenylindole Dihydrochloride (DAPI), 1,3-Diphenylisobenzofuran (DBPF), hydrazine monohydrate, thionyl chloride, palladium on activated charcoal (Pd/C), potassium ferricyanide was obtained from Aladdin (China). Other chemicals were of analytical grade and used without further purification.

4.2 Synthesis of Gan-ZnPc

Detailed synthesis procedure was seen in supplementary data.

4.3 Characterization of Gan-ZnPc

UV-vis Spectroscopy. ZnPc, Ganetespib, Gan-ZnPc were dissolved in DMSO at 5 μM . The UV-visible absorption spectra from 200 nm to 900 nm were acquired with an UV-vis spectrophotometer (TECHCOMP, UV2600 spectrophotometer).

Fluorescence Spectroscopy. ZnPc and Gan-ZnPc were dissolved in DMSO at 3 μM and their fluorescence spectra were acquired with a spectrofluorophotometer (Fluoromax-4, Horiba, Japan). The fluorescence spectroscopy of Gan-ZnPc in aqueous solution was obtained similarly. Briefly, Gan-ZnPc was dissolved in PBS

containing 1% (V/V) DMSO, then the exact volume of FBS (fetal bovine serum) was added. The fluorescence spectroscopy in aqueous solution was expressed by normalized emission intensity. The fluorescence excitation spectra of ZnPc and Gan-ZnPc were acquired through monitoring emission wavelength at 780 nm. The fluorescence emission spectra were acquired by exciting at 560 nm.

Detection of ROS. The generation of ROS was detected using DBPF as a ROS indicator. DBPF can capture and react with ROS rapidly, leading the decreased absorbance at 416 nm. Therefore, the generation of ROS was demonstrated by the characteristic absorbance decrease of DPBF at 416 nm. The stock solution of DBPF (60 μM) in DMSO was added blank DMSO as control, ZnPc or Gan-ZnPc at a final concentration at 1 μM . Then, the mixture was exposed to laser irradiation at 671 nm (20 mW cm^{-2}) in an interval of 120 s and the absorbance at 416 nm was detected per 10 s. The generation of ROS of Gan-ZnPc in aqueous solution was acquired using the same method. In brief, DBPF and Gan-ZnPc was dissolved in PBS containing 1% (V/V) DMSO, then the exact volume of FBS was added. The mixture was exposed to laser irradiation and the absorbance at 416 nm was detected per 20 s. The DBPF degradation was calculated as $(A_0 - A_t)/A_0 \times 100\%$ (A_t : the absorbance of the mixture solution at specified time after irradiation; A_0 : the absorbance of the mixture solution before irradiation)

Photostability. The photostability of ZnPc and Gan-ZnPc after irradiation was detected by the decrease of their characteristic absorption. ZnPc and Gan-ZnPc was

dissolved in DMSO at 5 μM and exposed to laser irradiation at 671 nm (100 mW cm^{-2}) in an interval of 20 min. The characteristic absorption, 672 nm for ZnPc and 678 nm for Gan-ZnPc, was detected per 2 min. And the photostability was calculated as A_t/A_0 . (A_t : the characteristic absorption of the solution at specified time after irradiation; A_0 : the characteristic absorption of the solution before irradiation)

4.4 Cellular assay

Cell culture. MCF7 human breast cancer cells, 4T1 murine breast cancer cells, NIH/3T3 murine embryonic fibroblast cells were obtained from Laboratory Animal Center of Sun Yat-sen University (Guangzhou, China) and cultured in RPMI 1640 or DMEM containing 10% FBS and antibiotics (penicillin 100 U mL^{-1} and streptomycin 100 $\mu\text{g mL}^{-1}$) under a humidified atmosphere at 37 °C with 5% CO_2 . During the cell assay experiments, drugs were dissolved in culture medium containing 0.5% DMSO and 10% FBS.

Cellular Uptake (determined by confocal CLSM). MCF7 or NIH/3T3 cells were seeded at glass base dish and incubated overnight. The culture medium was removed and rinsed twice with PBS, then the cells were incubated with a solution of ZnPc or Gan-ZnPc, Gan-ZnPc/Ganetespib (1/100, n/n) at a concentration of 1 μM for 2 h or 4 h under the same conditions. After that, the solution was removed and the cells were washed twice with PBS and dyed with DAPI. Then, cells were washed 5 times with PBS and imaged with CLSM (LSM 710, Zeiss, Germany).

Cellular Uptake (determined by FCM analysis). MCF7 or NIH/3T3 cells were incubated in 24-well plates overnight. The medium was removed and rinsed twice with PBS, the cells were washed with PBS, then the cells were incubated with a solution of ZnPc or Gan-ZnPc, Gan-ZnPc/Ganetespib (1/100, n/n) for 4 h under the same conditions. After removing the solution and rinsing with PBS, cells were harvested and resuspended in PBS for flow cytometry measurements. (Guava EasyCyte 6-2L, Merck Millipore).

Intracellular ROS generation. MCF7 cells or NIH/3T3 cells were seeded at glass base dish overnight. The medium was removed and rinsed twice with PBS, then the solution of ZnPc or Gan-ZnPc, Gan-ZnPc/Ganetespib (1/100, n/n) was added. After 4 h incubation, the solution was removed and further incubated with DCFH-DA for 30 min and then exposed to red light irradiation (50 mW cm^{-2} , 660-670 nm) for 5 min. Then, the cells were washed with PBS and dyed with DAPI following imaged with CLSM.

In vitro Cytotoxicity Study. The in vitro cytotoxicity of Ganetespib, ZnPc and Gan-ZnPc against MCF7, 4T1 or NIH/3T3 cells for 24 h, 48 h and 72 h were determined by MTT assay. Ganetespib, ZnPc, Ganetespib/Gan-ZnPc (equimolar mixture) and Gan-ZnPc were first dissolved in DMSO and diluted with culture medium to get different concentration solution with contained 0.5% DMSO. Cells were incubated in 96-well plates (5×10^4 cells per well) with 100 μL DMEM contain 10% FBS overnight at 37 °C with 5% CO_2 . The medium was removed and rinsed

twice with PBS, then 100 μ L of drug solution or culture medium containing 0.5% DMSO as control was added and incubated for determinate time. For the first group that total incubation time was 24 h, cells were first incubated for 6 h with drug solutions. After drug solution was removed, cells were rinsed with PBS and fresh culture medium was added. Cells were exposed for red light irradiation (100 mW cm^{-2} , 660-670 nm) for 10 min and then continuously incubated in incubator. The same red-light irradiation (same intensity, same wavelength and same irradiation time) were then exposed to cells at 9 h and 12 h, and then cells were incubated in incubator for another 12 h, before MTT solution was added. The total incubation time was 48 h for the second group, the cells were first incubated for 12 h with drug solutions rinsed with PBS followed by adding fresh culture medium. The same red-light irradiation was also exposed to cells at 12 h, 18 h and 24 h. Then the cells were incubated in incubator for another 24 h. For the third group with the total incubation time of 72 h, in which the cells were first incubated for 24 h with drug solutions and then rinsed with PBS followed by added fresh culture medium. The same red-light irradiation was exposed to cells at 24 h, 30 h and 36 h. Then the cells were incubated in incubator for another 36 h. Cytotoxicity for 24 h, 48 h and 72 h without irradiation was carried out similarly. In brief, cells were incubated with drug solution and rinsed with PBS at 6 h, 12 h, 24 h, respectively. Then fresh culture medium was added and cells were continually incubated till the time achieved. When the incubation was completed, MTT solution was added and incubated for another 4h, then the culture medium was

replaced with DMSO. The cell viability was measured with a microplate reader (ELX800, Bio-Tek, USA) by the percentage of optical density value at 490 nm.

4.5 In vivo assay

Animals and tumor model. Female BALB/c mice (20 ± 2 g, 5–6 weeks) were obtained from the Laboratory Animal Center of Sun Yat-sen University (Guangzhou, China). All experimental procedures were approved and supervised by the Institutional Animal Care and Use Committee of Sun Yat-sen University.

To develop the breast tumor model, the 4T1 cell suspension (1×10^6 cells) was subcutaneously injected into the right flank of each mouse. Tumor volumes were calculated according to the formula: $(L \times W^2)/2$, (L is the longest and W is the shortest tumor diameter (mm)).

In vivo biodistribution. 4T1 bearing BALB/c mice were randomly divided into two groups ($n=3$) and received a single intravenous injection of ZnPc and Gan-ZnPc (both at a dosage of $0.5 \mu\text{mol kg}^{-1}$). Mice were anesthetized and imaged on the unhairing area directly at 1, 3, 6, 9, 12, 24 h via small animal imaging system (NightOWL LB983, Berthold, Germany, excitation: 630 nm, emission: 680 nm). After last imaged, they were sacrificed and hearts, livers, spleens, lungs, kidneys and tumors were excised for imaging. Mean fluorescence intensity (MFI) of excised major organs and tumor was calculated as fluorescence counts per square millimeter.

In vivo antitumor efficacy. When the tumor volume reached about 100 mm^3 , 4T1 bearing mice were divided randomly into 8 groups ($n = 6$) and treated with saline,

Ganetespib, ZnPc, Gan-ZnPc (both at a dosage of $0.5 \mu\text{mol kg}^{-1}$, 1% DMSO in saline as vehicle and as control) with and without laser irradiation (500 mW cm^{-2} , 671 nm) every four days. Then, the tumor regions of mice were exposed to laser irradiation for 10 min at 1, 4, 7 h respectively post intravenous injection. Tumor volume and body weight were recorded every two days. Upon completion of the PDT treatment, all the mice were sacrificed and all the tumors were excised and gathered for imaging and weighing.

4.6 Statistical analysis

Quantitative data were expressed as mean \pm standard deviation (SD). Student's t-test was used for statistical comparisons between the experimental group and control groups. Statistical Package for the Social Sciences version 19.0 (SPSS 19.0, SPSS Inc., USA) was used for statistical analyses. $p < 0.05$ was considered statistically significant, $p < 0.01$ and $p < 0.001$ were considered highly significant.

Note

The authors declare no conflict of interest.

Acknowledgements

We are grateful for financial support from the National Natural Science Foundation of China (grant number: 81673369/H3008) and Science and Technology Planning Key Project of Guangdong Province, China (grant number: 2015B020211005).

Supplementary data

Additional experimental procedures, detailed synthetic procedure and scheme; ^1H

NMR spectra and MALDI-TOF spectra characterization data; UV/Vis absorption spectra of DBPF under laser irradiation with Gan-ZnPc or ZnPc; ROS generation of Gan-ZnPc and ZnPc in aqueous solution; photobleaching of ZnPc and Gan-ZnPc; CLSM images of MCF7 cells and NIH/3T3 cells after incubation with ZnPc, Gan-ZnPc or Gan-ZnPc/GanetespiB mixture

Abbreviations

PDT: photodynamic therapy; PS: photosensitizer; ZnPc: zinc phthalocyanine; Hsp90: heat shock protein 90; ROS: reactive oxygen species; FBS: fetal bovine serum; DBPF: 1,3-Diphenylisobenzofuran; CLSM: confocal laser scanning microscopy; FCM: flow cytometry.

References

- [1] D.W. Felsher, Cancer revoked: oncogenes as therapeutic targets, *Nat. Rev. Cancer*, 3 (2003) 375-380.
- [2] C. Fabris, G. Valduga, G. Miotto, L. Borsetto, G. Jori, S. Garbisa, E. Reddi, Photosensitization with zinc (II) phthalocyanine as a switch in the decision between apoptosis and necrosis, *Cancer Res.*, 61 (2001) 7495-7500.
- [3] V.F. Otvagin, A.V. Nyuchev, N.S. Kuzmina, I.D. Grishin, A.E. Gavryushin, Y.V. Romanenko, O.I. Koifman, D.V. Belykh, N.N. Peskova, N.Y. Shilyagina, I.V. Balalaeva, A.Y. Fedorov, Synthesis and biological evaluation of new water-soluble photoactive chlorin conjugate for targeted delivery, *Eur. J. Med. Chem.*, 144 (2017) 740-750.
- [4] M. Abbas, Q. Zou, S. Li, X. Yan, Self-Assembled Peptide- and Protein-Based Nanomaterials for Antitumor Photodynamic and Photothermal Therapy, *Adv. Mater.*, 29 (2017).
- [5] M. Dichiaro, O. Prezzavento, A. Marrazzo, V. Pittala, L. Salerno, A. Rescifina, E. Amata, Recent advances in drug discovery of phototherapeutic non-porphyrinic anticancer agents, *Eur. J. Med. Chem.*, 142 (2017) 459-485.

- [6] F.L. Zhang, M.R. Song, G.K. Yuan, H.N. Ye, Y. Tian, M.D. Huang, J.P. Xue, Z.H. Zhang, J.Y. Liu, A Molecular Combination of Zinc(II) Phthalocyanine and Tamoxifen Derivative for Dual Targeting Photodynamic Therapy and Hormone Therapy, *J. Med. Chem.*, 60 (2017) 6693-6703.
- [7] W.M. Sharman, C.M. Allen, J.E. van Lier, Photodynamic therapeutics: basic principles and clinical applications, *Drug Discov. Today*, 4 (1999) 507-517.
- [8] T. Chatzisideri, S. Thysiadis, S. Katsamakas, P. Dalezis, I. Sigala, T. Lazarides, E. Nikolakaki, D. Trafalis, O.A. Gederaas, M. Lindgren, V. Sarli, Synthesis and biological evaluation of a Platinum(II)-c(RGDyK) conjugate for integrin-targeted photodynamic therapy, *Eur. J. Med. Chem.*, 141 (2017) 221-231.
- [9] S. Wilhelm, A.J. Tavares, Q. Dai, S. Ohta, J. Audet, H.F. Dvorak, W.C.W. Chan, Analysis of nanoparticle delivery to tumours, *Nat Rev Mater*, 1 (2016).
- [10] R.K. Jain, T. Stylianopoulos, Delivering nanomedicine to solid tumors, *Nat. Rev. Clin. Oncol.*, 7 (2010) 653-664.
- [11] F. Danhier, To exploit the tumor microenvironment: Since the EPR effect fails in the clinic, what is the future of nanomedicine?, *J. Control. Release*, 244 (2016) 108-121.
- [12] M. Srinivasarao, C.V. Galliford, P.S. Low, Principles in the design of ligand-targeted cancer therapeutics and imaging agents, *Nat. Rev. Drug Discov.*, 14 (2015) 203-219.
- [13] M. Srinivasarao, P.S. Low, Ligand-Targeted Drug Delivery, *Chem. Rev.*, 117 (2017) 12133-12164.
- [14] J.T.F. Lau, P.-C. Lo, W.-P. Fong, D.K.P. Ng, A Zinc(II) Phthalocyanine Conjugated with an Oxaliplatin Derivative for Dual Chemo- and Photodynamic Therapy, *J. Med. Chem.*, 55 (2012) 5446-5454.
- [15] M.R. Ke, S.F. Chen, X.H. Peng, Q.F. Zheng, B.Y. Zheng, C.K. Yeh, J.D. Huang, A tumor-targeted activatable phthalocyanine-tetrapeptide-doxorubicin conjugate for synergistic chemo-photodynamic therapy, *Eur. J. Med. Chem.*, 127 (2017) 200-209.

- [16] Z. Huang, L. Huang, Y. Huang, Y. He, X. Sun, X. Fu, X. Xu, G. Wei, D. Chen, C. Zhao, Phthalocyanine-based coordination polymer nanoparticles for enhanced photodynamic therapy, *Nanoscale*, 9 (2017) 15883-15894.
- [17] P. Xu, Y. Jia, Y. Yang, J. Chen, P. Hu, Z. Chen, M. Huang, Photodynamic Oncotherapy Mediated by Gonadotropin-Releasing Hormone Receptors, *J. Med. Chem.*, 60 (2017) 8667-8672.
- [18] T. Shimamura, S.A. Perera, K.P. Foley, J. Sang, S.J. Rodig, T. Inoue, L. Chen, D. Li, J. Carretero, Y.C. Li, P. Sinha, C.D. Carey, C.L. Borgman, J.P. Jimenez, M. Meyerson, W. Ying, J. Barsoum, K.K. Wong, G.I. Shapiro, Ganetespib (STA-9090), a nongeldanamycin HSP90 inhibitor, has potent antitumor activity in in vitro and in vivo models of non-small cell lung cancer, *Clin. Cancer. Res.*, 18 (2012) 4973-4985.
- [19] A. Kamal, L. Thao, J. Sensintaffar, L. Zhang, M.F. Boehm, L.C. Fritz, F.J. Burrows, A high-affinity conformation of Hsp90 confers tumour selectivity on Hsp90 inhibitors, *Nature*, 425 (2003) 407-410.
- [20] L. Whitesell, S.L. Lindquist, HSP90 and the chaperoning of cancer, *Nat. Rev. Cancer*, 5 (2005) 761-772.
- [21] D. Picard, Hsp90 invades the outside, *Nat. Cell Biol.*, 6 (2004) 479-480.
- [22] B.K. Eustace, T. Sakurai, J.K. Stewart, D. Yimlamai, C. Unger, C. Zehetmeier, B. Lain, C. Torella, S.W. Henning, G. Beste, B.T. Scroggins, L. Neckers, L.L. Ilag, D.G. Jay, Functional proteomic screens reveal an essential extracellular role for hsp90 alpha in cancer cell invasiveness, *Nat. Cell Biol.*, 6 (2004) 507-514.
- [23] Y.S. Kim, S.V. Alarcon, S. Lee, M.J. Lee, G. Giaccone, L. Neckers, J.B. Trepel, Update on Hsp90 Inhibitors in Clinical Trial, *Curr Top Med Chem*, 9 (2009) 1479-1492.
- [24] F.H. Schopf, M.M. Biebl, J. Buchner, The HSP90 chaperone machinery, *Nat. Rev. Mol. Cell Biol.*, 18 (2017) 345-360.
- [25] W. Ying, Z. Du, L. Sun, K.P. Foley, D.A. Proia, R.K. Blackman, D. Zhou, T. Inoue,

- N. Tatsuta, J. Sang, S. Ye, J. Acquaviva, L.S. Ogawa, Y. Wada, J. Barsoum, K. Koya, Ganetespib, a unique triazolone-containing Hsp90 inhibitor, exhibits potent antitumor activity and a superior safety profile for cancer therapy, *Mol. Cancer Ther.*, 11 (2012) 475-484.
- [26] L.B. Crowe, P.F. Hughes, D.A. Alcorta, T. Osada, A.P. Smith, J. Totzke, D.R. Loiselle, I.D. Lutz, M. Gargasha, D. Roy, J. Roques, D. Darr, H.K. Lyerly, N.L. Spector, T.A.J. Haystead, A Fluorescent Hsp90 Probe Demonstrates the Unique Association between Extracellular Hsp90 and Malignancy in Vivo, *ACS Chem. Biol.*, 12 (2017) 1047-1055.
- [27] J.J. Barrott, P.F. Hughes, T. Osada, X.Y. Yang, Z.C. Hartman, D.R. Loiselle, N.L. Spector, L. Neckers, N. Rajaram, F. Hu, N. Ramanujam, G. Vaidyanathan, M.R. Zalutsky, H.K. Lyerly, T.A. Haystead, Optical and radioiodinated tethered Hsp90 inhibitors reveal selective internalization of ectopic Hsp90 in malignant breast tumor cells, *Chem. Biol.*, 20 (2013) 1187-1197.
- [28] X. Wang, X. Song, W. Zhuo, Y. Fu, H. Shi, Y. Liang, M. Tong, G. Chang, Y. Luo, The regulatory mechanism of Hsp90 α secretion and its function in tumor malignancy, *Proc. Natl. Acad. Sci. U. S. A.*, 106 (2009) 21288-21293.
- [29] J. Sun, X. Ren, J.W. Simpkins, Sequential Upregulation of Superoxide Dismutase 2 and Heme Oxygenase 1 by tert-Butylhydroquinone Protects Mitochondria during Oxidative Stress, *Mol. Pharmacol.*, 88 (2015) 437-449.
- [30] A. Ferrario, C.J. Gomer, Targeting the 90 kDa heat shock protein improves photodynamic therapy, *Cancer Lett.*, 289 (2010) 188-194.
- [31] T.Y. Lin, W. Guo, Q. Long, A. Ma, Q. Liu, H. Zhang, Y. Huang, S. Chandrasekaran, C. Pan, K.S. Lam, Y. Li, HSP90 Inhibitor Encapsulated Photo-Theranostic Nanoparticles for Synergistic Combination Cancer Therapy, *Theranostics*, 6 (2016) 1324-1335.
- [32] Y. Yuan, J. Liu, B. Liu, Conjugated-polyelectrolyte-based polyprodrug: targeted and image-guided photodynamic and chemotherapy with on-demand drug release

upon irradiation with a single light source, *Angew. Chem. Int. Ed. Engl.*, 53 (2014) 7163-7168.

- [33] D. Matulis, I. Cikotiene, E. Kazlauskas, J. Matuliene, 5-Aryl-4-(5-substituted 2, 4-dihydroxyphenyl)-1, 2, 3-thiadiazoles as inhibitors of HSP90 chaperone and the intermediates for production thereof, WO2009134110, 2009.
- [34] E.L. Spitler, W.R. Dichtel, Lewis acid-catalysed formation of two-dimensional phthalocyanine covalent organic frameworks, *Nat. Chem.*, 2 (2010) 672-677.
- [35] M.K. Kuimova, H.A. Collins, M. Balaz, E. Dahlstedt, J.A. Levitt, N. Sergent, K. Suhling, M. Drobizhev, N.S. Makarov, A. Rebane, H.L. Anderson, D. Phillips, Photophysical properties and intracellular imaging of water-soluble porphyrin dimers for two-photon excited photodynamic therapy, *Org. Biomol. Chem.*, 7 (2009) 889-896.

A Tumor-targeted Ganetespib-Zinc Phthalocyanine Conjugate for Synergistic Chemo-Photodynamic Therapy

Liangfeng Huang,[‡] Gaofei Wei,^{‡} Xiaoqi Sun, Yali Jiang, Zeqian Huang, Yanjuan Huang, Yifeng Shen, Xiaoyu Xu, Yunhui Liao and Chunshun Zhao**

School of Pharmaceutical Sciences, Sun Yat-sen University, Guangzhou, 510006,
People's Republic of China

*Corresponding Author: E-mail: zhaocs@mail.sysu.edu.cn, Tel: +86 20 39943118

Highlights

- Gan-ZnPc was developed by conjugating zinc phthalocyanine with Ganetespib.
- It was bound to Hsp90 and then selectively internalized into the tumor cells.
- The concentrated intracellular photosensitizer enhanced photodynamic therapy.
- It can inhibit Hsp90 and integrate photodynamic therapy in a synergistic manner.
- Gan-ZnPc implemented tumor selectivity, photodynamic therapy and chemotherapy simultaneously.